(Received 8 August 2024, Accepted 14 September 2024, Scheduled 30 September 2024)

Study of an Electric Vehicle WPT System with Ring-Series Passive Magnetic Shielding Based on Dual Transmitting Coils

Xueyi Zhang[1], Zhibang Luo[1], Sai Zhang[1], Bin Li[1], Ziyue Gan[1], and Zhongqi Li[1, 2, 3, *]

[1] College of Electrical and Information Engineering, Hunan University of Technology, Zhuzhou 412007, China
[2] College of Electrical and Information Engineering, Hunan University, Changsha 412008, China
[3] College of Railway Transportation, Hunan University of Technology, Zhuzhou 412007, China

ABSTRACT: In the design of wireless power transfer (WPT) systems for electric vehicles, minimizing magnetic leakage while maintaining high transmission efficiency is a challenging problem. To this end, a novel structure featuring dual transmitting coils and a ring-series magnetic shielding coil (RMSDT) is proposed to reduce magnetic leakage during system charging, thereby enhancing system safety performance. Additionally, the Particle Swarm Optimization (PSO) algorithm is employed to optimize system parameters, aiming to achieve high transmission efficiency while maintaining low magnetic leakage. To validate the effectiveness of the proposed design, a shielded WPT system for electric vehicles has been developed. Its performance is verified through a combination of experiments and simulations. The results demonstrate that the PSO algorithm significantly enhances transmission efficiency compared to traditional optimization methods. At an output power of 3.7 kW, the peak transmission efficiency exceeds 95%, representing an improvement of 4.63% compared to the conventional for-loop algorithm. Furthermore, the leakage magnetic field of the RMSDT structure in the target region is only 16.08 μT, which is effectively reduced by 41.8% compared to the conventional WPT structure and sacrifices only 0.21% transmission efficiency. In summary, this paper can provide some references to the safety and efficiency of electric vehicle WPT.

1. INTRODUCTION

As science and technology progress, the world is moving towards more convenient and efficient operations. In the 21st century, the electric power industry has been constantly industrializing, marking the beginning of a new era of electric power. Traditional contact-based power transmission methods have many drawbacks, such as safety issues and inconvenience in practical application. To address these problems, wireless power transfer (WPT) technology has emerged [1–4]. As WPT technology matures and becomes more integrated into our lives, the potential applications are expanding rapidly. WPT technology has been recognized by the World Economic Forum (WEF) as one of the top ten emerging technologies for two consecutive years. It has been highlighted for its significant impact on the world and its potential to offer solutions to global challenges. [5–8]. Usually, WPT technology is used in electric vehicles, cell phones, medical devices, drones, and other applications [9–12]. However, magnetic leakage is an inevitable issue when using WPT technology, which can be harmful to the human body and devices. In the charging process of electric vehicles, large power requirements can lead to more significant magnetic leakage than other scenarios. As new energy technologies continue to advance, electric vehicles are likely to become the mainstream choice, making it crucial to limit magnetic leakage during charging. However, simply reducing magnetic leakage can negatively impact charging efficiency, affecting the convenience for users. Therefore, it is important to focus on minimizing magnetic leakage while maintaining high transmission efficiency.

Electromagnetic shielding technology has emerged as a prominent research hotspot in the field of magnetic coupling resonant wireless power transfer (MCRWPT) [13, 14]. Researchers have extensively explored and made significant contributions to the development of electromagnetic shielding for WPT systems.

As early as 2000, the Dickinson team at the Jet Propulsion Laboratory in the U.S. began to pay attention to the safety of electromagnetic applications [15]. Subsequently, in 2007, for the safety of MCRWPT electromagnetic environment, an MIT team was very forward-looking to assess and analyze it [16]. The Hirayama team of Nagoya Institute of Technology (NIT), Japan, was precisely influenced by the former and also studied the experiments on the safety of human electromagnetic environment in 2012 [17]. By 2019, the KAIST (Korea Advanced Institute of Science and Technology) team improved the safety of the WPT system of smartwatches for the human body by studying electromagnetic shielding, and in 2020 and 2022, the team continued to make further improvements in reducing the magnetic leakage of drones and proposed a shielding method for independent power supplies [18–20]. In China, the research on electromagnetic shielding has also been gradually developing in recent years, with teams from Southeast University, South China University of Technology, and Southwest Jiaotong

* Corresponding author: Zhongqi Li (my3eee@126.com).

University conducting comprehensive research on electromagnetic environments and electromagnetic compatibility [21, 22].

For MCRWPT systems, there are two typical shielding methods: passive shielding and active shielding. Active shielding involves a more complex structure and circuit design, as it requires an excitation source for the suppression coil to generate an opposing magnetic field that offsets the leakage field. This method demands intricate coordination between the suppression coil and the main circuit. Meanwhile, the coupling of the suppression coil with the main circuit can lead to a reduction in the coupling coefficient between the transmitting and receiving coils, thereby affecting the system's transmission performance. When the suppression coil is not directly involved in the main magnetic circuit, its impact on transmission performance is minimized, leading to a more efficient overall system, hence passive shielding does not directly interfere with the main magnetic circuit of the WPT system. This approach relies on materials and configurations, which naturally block or redirect the unwanted magnetic fields without requiring additional power or active components. As a result, passive shielding may be a more effective magnetic field shielding method while maintaining the maneuverability of the power transfer system. This makes passive shielding a preferable option in many scenarios where reliability is paramount [23, 24].

A passive shielding structure was proposed in [25], which is very innovative and commercial, but its effectiveness in reducing magnetic leakage is limited due to the predominant use of aluminum to cut costs. Therefore, it is necessary to design the system structure to strengthen the counteracting magnetic field between coils. Lee and other scholars, from the KAIST, proposed a novel hybrid loop array structure that combines a reactive shielding coil and an amplifying coil. Although this structure can effectively carry out magnetic leakage shielding and also strengthen the magnetic coupling reaction between the transmitting coil and receiving coil, it sacrifices a lot of transmission efficiency, which will be difficult to apply to the actual scene [26]. Thus, it can be seen that although the multi-coil array can be better designed structurally, it needs to be used in appropriate aspects to take into account the transmission efficiency. A dual shielding coils structure is proposed in [27], and the adopted multi-coil active shield significantly reduce the magnetic field in critical areas. However, since there are two active shielding coils and one transmitting coil, and each of the three requires a power supply. A plurality of external power supplies are formed, which will make the system circuit become unstable and complex, and the system parameters become difficult to optimize.

In this paper, a novel structure with ring-series magnetic shielding based on dual transmitting (RMSDT) coils is proposed. This strong coupling coil structure can effectively reduce the magnetic leakage compared to traditional WPT systems. The use of multiple transmitting coils provides more design freedom to the system, offering greater flexibility in array arrangement and combination [28, 29]. This, in turn, can provide a broader solution space for realizing high efficiency and low magnetic leakage. Compared with the design of multiple active shielding coils, multi-transmitting coils can still maintain design diversity, but the circuit does not become overly complicated due to too many voltage sources. To optimize the RMSDT system, the Particle Swarm Optimization (PSO) algorithm is utilized. The PSO algorithm is an evolutionary optimization technique inspired by the random foraging behavior of bird flocks. It is simple to implement, highly accurate, and converges quickly, making it well suited for function optimization and various engineering design problems [30]. In this work, the PSO algorithm is utilized to determine the shielding coil matching capacitance and the load at the receiving end, thereby improving the transmission efficiency of the system. Finally, the accuracy of the results and the validity of the method are verified through simulation and experiment. Compared to the conventional WPT system, the RMSDT system achieves a 41.8% reduction in magnetic leakage with virtually no reduction in transmission efficiency. Compared to the traditional for-loop algorithm, the PSO algorithm can improve the transmission efficiency by 4.63% under the same structure. This demonstrates the RMSDT system's ability to be more environmentally friendly than conventional WPT systems, and the PSO algorithm can improve the transmission efficiency more remarkably than for-loop algorithm. Therefore, this paper provides ideas for the multi-coil design of electric vehicle WPT charging system structures and the optimization of system parameters. Future WPT research can also be expanded to multi-coil arrays and optimization algorithms, making the methods to achieve the goals more diversely.

2. COIL MAGNETIC FIELD CALCULATION

To calculate the magnetic field distribution in space, a vector magnetic potential-based approach for rectangular coils is introduced [31]. Figure 1 illustrates the spatial position, and a_1 and a_2 denote the half-length and half-width of the coil. Therefore, the perpendicular distance between receiving coil and transmitting coil is denoted as Z_0 and the current flowing through the receiving coil as I.

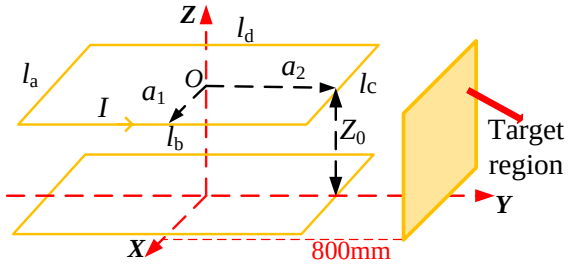

FIGURE 1. Schematic diagram of coil unit.

Assuming that the current density of the current-carrying conductor in air is J, the magnetic vector potential expression generated at any point $P(x, y, z)$ is as follows:

$$A(x, y, z) = \frac{\mu_0}{4\pi} \int_v \frac{J(x', y', z')\, dv'}{R} \tag{1}$$

where V is the current distribution in the conductor, and R is the distance between any point $P(x, y, z)$ and the point source

(x', y', z'), which can be expressed as:

$$R=\sqrt{(x-x')^2+(y-y')^2+(z-z')^2} \tag{2}$$

the above equation is solved by the double Fourier transform as follows:

$$b(\xi,\eta,z)=\int_{-\infty}^{\infty}\int_{-\infty}^{\infty}B(x,y,z)\cdot e^{-j(x\xi+y\eta)}dxdy \tag{3}$$

$$B(x,y,z)=\frac{1}{4\pi^2}\int_{-\infty}^{\infty}\int_{-\infty}^{\infty}b(\xi,\eta,z)\cdot e^{j(x\xi+y\eta)}d\xi d\eta \tag{4}$$

where ξ and η are double Fourier integral variables, and the magnetic induction strength components of a single coil are obtained:

$$B=\nabla\times A \tag{5}$$

$$B_x=\frac{1}{4\pi^2}\int_{-\infty}^{\infty}\int_{-\infty}^{\infty}\frac{j2\mu_0 I sin(\xi a_1)\, sin(\eta a_2)}{\eta}e^{j(x\xi+y\eta)}d\xi d\eta \tag{6}$$

$$B_y=\frac{1}{4\pi^2}\int_{-\infty}^{\infty}\int_{-\infty}^{\infty}\frac{j2\mu_0 I sin(\xi a_2)\, sin(\eta a_1)}{\xi}e^{j(x\xi+y\eta)}d\xi d\eta \tag{7}$$

$$B_z=\frac{-1}{4\pi^2}\int_{-\infty}^{\infty}\int_{-\infty}^{\infty}\frac{2\mu_0 I q sin(\xi a_1)\, sin(\eta a_2)}{\xi\eta}e^{j(x\xi+y\eta)}d\xi d\eta \tag{8}$$

therefore, the magnetic induction can be expressed as:

$$B=\sqrt{{B_x}^2+{B_y}^2+{B_z}^2} \tag{9}$$

3. RMSDT STRUCTURE

As mentioned earlier, multiple transmitting coils are used in this paper. For the shielding coil, four coils are connected in series. Compared with the traditional single rectangular coil, the shielding coil in this paper offers greater flexibility in placement. However, since the four coils are connected in series, they still function as a single coil in the system. Therefore, the shielding coil in this paper does not complicate the circuit while increasing the spatial design dimension.

An RMSDT structure consists of two identical transmitting coils, denoted as T_{x1} and T_{x2}, a receiving coil (R_x), and a single shielding coil (S_c). The transmitting coils are positioned at the same level, as the shielding coil, and the specific structural model is depicted in Figures 2 and 3. In Figure 2, S_c is divided into four components: S_{c1}, S_{c2}, S_{c3}, and S_{c4}, and these four components are connected in series to form a complete S_c structure. The distance between a single transmitting coil and the shielding coil in the Y-axis direction is denoted as b_1; the distance between the transmitting coil and shielding coil in the X-axis direction is denoted as b_2; and the distance between the two transmitting coils is denoted as b_3. In Figure 3, the currents flowing through these coils are designated as I_1, I_2, I_3, and I_4, corresponding to the currents in T_{x1}, T_{x2}, S_c, and R_x, respectively.

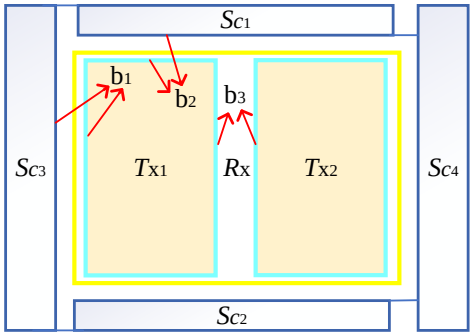

FIGURE 2. Schematic diagram of RMSDT Structure top view.

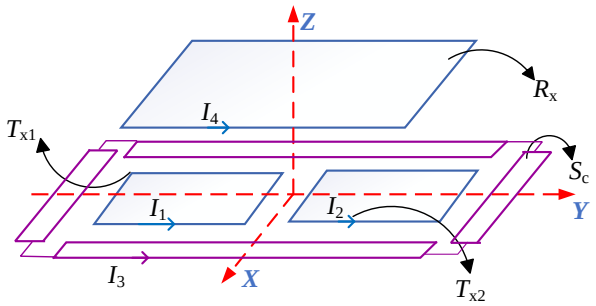

FIGURE 3. Schematic diagram of RMSDT structure.

The shielding principle of the RMSDT system is illustrated in Figure 4. In this configuration, T_{x1} and T_{x2} are surrounded by S_c. When the transmitting and receiving coils produce a leakage flux, the shielding coil intercepts this flux. As a result, an induced voltage (V_{ind}) is generated in the shielding coil, which can be expressed as:

$$V_{ind}=\int E\cdot dl=-\frac{d\phi}{dt}=-\frac{dB\cdot S}{dt} \tag{10}$$

where B is the time-varying leakage magnetic field generated by the transmitting and receiving coils, which can be expressed as:

$$B=B_0e^{j\omega t}=B_0\cos\omega t+jB_0\sin\omega t \tag{11}$$

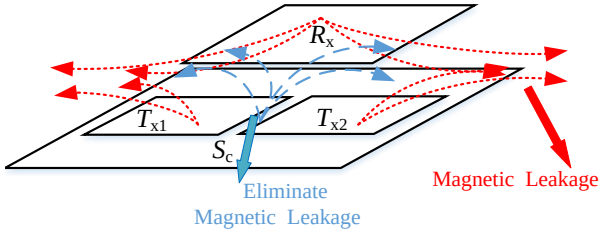

FIGURE 4. Magnetic shielding schematic.

The shielding coil internal resistance R_3 could be considered negligible,so the current in S_c can be expressed as:

$$I_3 = \frac{-j\omega B_0 e^{j\omega t} S}{j\omega L_3 - \frac{1}{\omega C_3}} \tag{12}$$

According to Biot-Savart's law, the counteracting magnetic field generated by the shielding coil can be expressed as:

$$B' = -B \cdot \frac{\mu_0 j\omega S}{4\pi j(\omega L_3 - \frac{1}{\omega C_3})} \int_{c'} \frac{\overrightarrow{dl} \times \overrightarrow{R}}{{R_3}^3} \tag{13}$$

It is not difficult to see that when the matching capacitance of S_c is greater than the resonant capacitance, the leakage magnetic field and counteracting magnetic field are reversed, which can have a shielding effect.

3.1. Equivalent Circuit and Mathematical Model of the RMSDT System

The equivalent circuit of the RMSDT structure in Figure 3 is depicted in Figure 5. In this equivalent circuit: the self-inductance of each coil is denoted as L_1, L_2, L_3, L_4; the equivalent resistance of each coil is denoted as R_1, R_2,R_3, R_4; the load of R_x is denoted as R_L; the mutual inductance between the coils is denoted as M_{12}, M_{13}, M_{14}, M_{23}, M_{24}, M_{34}; the resonant capacitance of the transmitting coils is denoted as C_1, C_2; the resonant capacitance of R_x is denoted as C_4; the applied matching capacitance of S_c is denoted as C_3. Based on the equivalent circuit model in Figure 5, the Kirchhoff voltage matrix of the system can be expressed as follows:

$$\begin{bmatrix} Z_1 & j\omega M_{12} & j\omega M_{13} & j\omega M_{14} \\ j\omega M_{21} & Z_2 & j\omega M_{23} & j\omega M_{24} \\ j\omega M_{31} & j\omega M_{32} & Z_3 & j\omega M_{34} \\ j\omega M_{41} & j\omega M_{42} & j\omega M_{43} & Z_4 \end{bmatrix} \begin{bmatrix} I_1 \\ I_2 \\ I_3 \\ I_4 \end{bmatrix} = \begin{bmatrix} V_{S1} \\ V_{S2} \\ 0 \\ 0 \end{bmatrix} \tag{14}$$

Where the input voltages of T_{x1}, T_{x2} are denoted as V_{s1}, V_{s2}, respectively, and R_s is the internal resistance of power supply. Since the two transmitting coils have the same dimensional parameters and are in a perfectly symmetrical position in the system, let $V_{s1} = V_{s2} = V_s$, and the impedance of T_{x1}, T_{x2}, S_c, and R_x is denoted as Z_1, Z_2, Z_3, and Z_4, respectively, when the system is in the resonance state, $Z_1 = R_1 + R_s$, $Z_2 = R_2 + R_s$, $Z_3 = R_3 + j\omega L_3 - 1/j\omega C_3$, $Z_4 = R_4 + R_L$.

It is known that I_1, I_2, I_3, and I_4 denote the currents in T_{x1}, T_{x2}, S_c, and R_x, respectively, so the currents and transmission efficiency can be expressed as Eq. (15) according to Eq. (14):

$$\begin{cases} I_1 = \dfrac{V_S}{j\omega M_{12}(1+AB) + R_1 - [j\omega M_{13}(M_{14}+M_{24}) + AM_{13}(Bj\omega M_{24} + R_4 + R_L)]/M_{34} + Aj\omega M_{14}} \\ I_2 = \dfrac{(1+AB)V_S}{j\omega M_{12}(1+AB) + R_1 - [j\omega M_{13}(M_{14}+M_{24}) + AM_{13}(Bj\omega M_{24} + R_4 + R_L)]/M_{34} + Aj\omega M_{14}} \\ I_3 = \dfrac{[j\omega(M_{14}+M_{24}) + A(Bj\omega M_{24} + R_4 + R_L)]V_S}{\omega^2 M_{12}M_{34}(1+AB) - j\omega M_{34}R_1 + [Aj\omega M_{13}(Bj\omega M_{24} + R_4 + R_L) - \omega^2 M_{13}(M_{14}+M_{24})] + A\omega^2 M_{14}M_{34}} \\ I_4 = \dfrac{AV_S}{j\omega M_{12}(1+AB) + R_1 - [j\omega M_{13}(M_{14}+M_{24}) + AM_{13}(Bj\omega M_{24} + R_4 + R_L)]/M_{34} + Aj\omega M_{14}} \\ A = \dfrac{2j\omega M_{13} - Z_3(M_{14}+M_{24})/M_{34}}{B(j\omega M_{23} - Z_3 M_{24}/M_{34}) - Z_3(R_4+R_L)/j\omega M_{34} + j\omega M_{34}} \\ B = \dfrac{j\omega M_{24} - j\omega M_{14}}{j\omega M_{12} - R_1} \\ \eta = \dfrac{{I_4}^2 R_L}{V_S(I_1+I_2)} \end{cases} \tag{15}$$

3.2. Equivalent Circuit and Mathematical Model of Conventional WPT System

A conventional WPT system generally consists of a single transmitting coil equipped with a receiving coil, as shown in the coil structure in Figure 6. In this configuration, T_x' is the transmitting coil, and R_x' is the receiving coil. The equivalent circuit model of this coil structure is depicted in Figure 7, where L_1', R_1' denote the self-inductance and the equivalent resistance of T_x'; L_2', R_2' denote the self-inductance and equivalent resistance of R_x', respectively; M denotes the mutual inductance between the coils; and R_L denotes the receiving coil load. Based on the equivalent circuit, it can be concluded that the Kirchhoff voltage matrix of the conventional WPT system is as follows:

$$\begin{bmatrix} {Z_1}' & j\omega M \\ j\omega M & {Z_2}' \end{bmatrix} \begin{bmatrix} {I_1}' \\ {I_2}' \end{bmatrix} = \begin{bmatrix} V_S' \\ 0 \end{bmatrix} \tag{16}$$

where V_S' denotes the input voltage; Z_1' and Z_2' denote the impedance of T_x' and R_x', respectively, and $Z_1' = R_1' + R_s$, $Z_2' = R_2'$, when the system is in the resonance state.

It is known that I_1', I_2' represent the currents in the coils, and the currents expression and transmission efficiency can be ob-

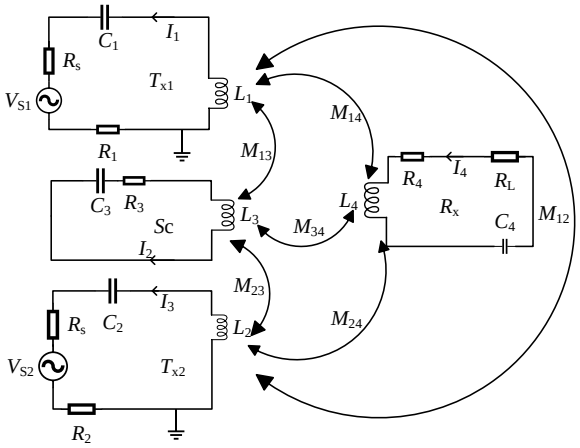

FIGURE 5. Equivalent circuit model of RMSDT structure.

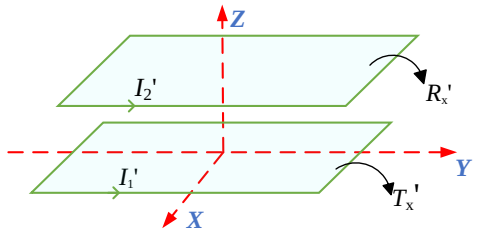

FIGURE 6. Schematic diagram of conventional WPT structure.

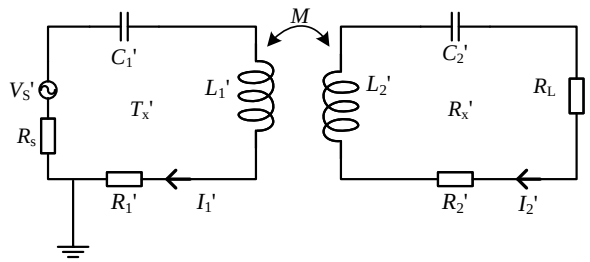

FIGURE 7. Equivalent circuit model of conventional WPT structure.

tained as:

$$I_1' = \frac{Z_2' V_S'}{Z_1' Z_2' + (\omega M)^2} \tag{17}$$

$$I_2' = \frac{j\omega V_S'}{Z_1' Z_2' + (\omega M)^2} \tag{18}$$

$$\eta' = \frac{I_2'^2 R_L}{V_S' I_1'} \tag{19}$$

4. PARAMETERS OPTIMIZATION OF THE RMSDT SYSTEM

In this paper, the RMSDT system is proposed to solve the problem of magnetic field leakage in the vertical direction. Normally, if there is a metal shielding device in the system, the observation point of magnetic leakage is set at about 800 mm horizontally from the center of the vehicle. The receiving and transmitting coils of the system are set at the center of the vehicle's landing gear and parking space accordingly. At the same time, according to the electric vehicle wireless charging standard GB/T 38775 part 4 electromagnetic field safety specification for electric vehicles, the vertical magnetic leakage standard, the vertical height of 700 mm outside the vehicle is taken as the dividing line. The magnetic leakage in the range of 700 mm and above should not exceed 27 μT [32]. Therefore, from the two aspects mentioned above, the maximum leakage observation point of this paper is found out from the magnetic field distribution of the 700-mm height horizontal plane. The target region of electric vehicles is shown in Figure 8.

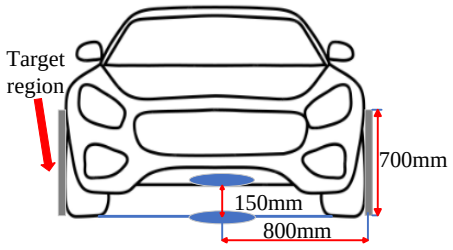

FIGURE 8. Target region of electric vehicles.

4.1. Optimization of the RMSDT Structure

In this subsection, a new optimization method is proposed to improve the system, and the optimization flowchart is shown in Figure 9. The specific steps are as follows:

(1) Setting of each coil size: Firstly, the wire selection of 3.96 mm outside diameter Litz copper wire and the size range of each coil are set, where the inner width and length of T_{x1} and T_{x2} range from 15 cm to 25 cm and 45 cm to 55 cm, respectively; the inner width and length of R_x both range from 45 cm to 55 cm; the inner width and length of the four parts of S_c are that the inner width of all the four ranges from 5 cm to 15 cm, and the inner length of S_{c1}, S_{c2} ranges from 60 cm to 70 cm, while the inner length of S_{c3}, S_{c4} ranges from 75 cm to 85 cm. Then, the number of turns for T_{x1}, T_{x2} and R_x are set between 10 and 20 turns, and the numbers of turns of S_{c1}, S_{c2}, S_{c3}, S_{c4} are set between 1 and 5 turns. The step of the number of turns is 1, and the step of widths and lengths is 1 cm.

(2) Setting of distance between coils: On the basis of the general electric vehicle charging device, the transmission distance between the transmitting coils and R_x is determined to be 15 cm. According to the RMSDT structure with strong symmetry, S_c is fixed in the same horizontal plane as the transmitting coils. The distance between T_{x1}, T_{x2} and S_c in the Y-axis direction (b_1), the distance between T_{x1}, T_{x2} and S_c in the X-axis direction (b_2), as well as the distance between T_{x1}, T_{x2} (b_3) as shown in Figure 2, are all set in the range of 1 cm to 5 cm with steps for 1 cm.

(3) Setting of the optimal capacitance of S_c and the optimal load of R_x: In this paper, the reasonable ranges for the load at R_x (R_L) and the capacitance of S_c (C_3) are from 10Ω to 40Ω and 1 nF to 1 mF, respectively. The transmission efficiency is calculated using Eqs. (6) to (9). If it is lower than 90%, the coil size and distance should be re-optimized in the previous

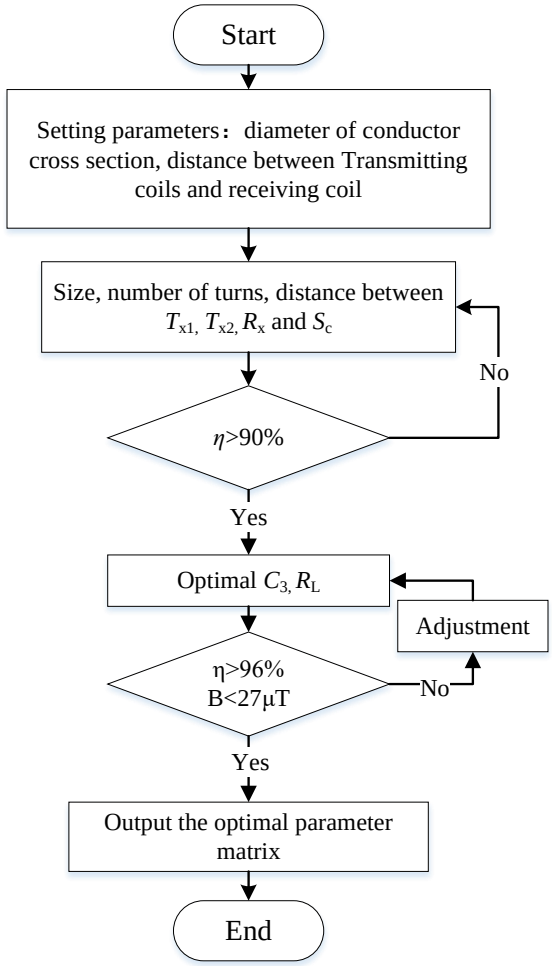

FIGURE 9. Overall optimization flowchart.

step; otherwise, R_L and C_3 are further optimized to continuously improve transmission efficiency. From Eqs. (6) to (9) and Eq. (15), it can be seen that the transmission efficiency and magnetic leakage are highly correlated with the R_L and C_3, so the transmission efficiency and magnetic leakage of the system could be ensured by controlling these two variables at the optimal values.

In this paper, the PSO algorithm is used to optimize C_3 and R_L. Firstly, the parameters of the PSO algorithm need to be initialized. The PSO algorithm is initialized with a group of random particles, and the optimal solution is then found through iteration. In each iteration, the particle updates itself by tracking two extreme values: body speed and position information. Since the independent variables in this paper are R_L and C_3, the particle dimension is set to 2. The number of iterations depends on the complexity of the problem, and with too few iterations the solution is unstable, while too many will waste time. Generally, it ranges from 100 to 4000 iterations, so this paper chooses 200. The inertia weight reflects the degree of influence of previous individuals on the present. In order to make the influence reasonable for each iteration, the inertia weight is set at 0.7. The learning factor depends on the value range of the independent variable. In this paper, the value ranges are not very large, and a learning factor ranging from 0 to 4 is generally suitable; therefore, a value of 1.5 is chosen for this study. The objective is to approach and converge to the solution of Eq. (14) throughout the iteration process in order to satisfy the voltage equation of the system. Additionally, a penalty function is introduced based on the output power, where a minimum output power of 3.7 kW must be achieved to proceed to the next iteration. The process is illustrated in Figure 10.

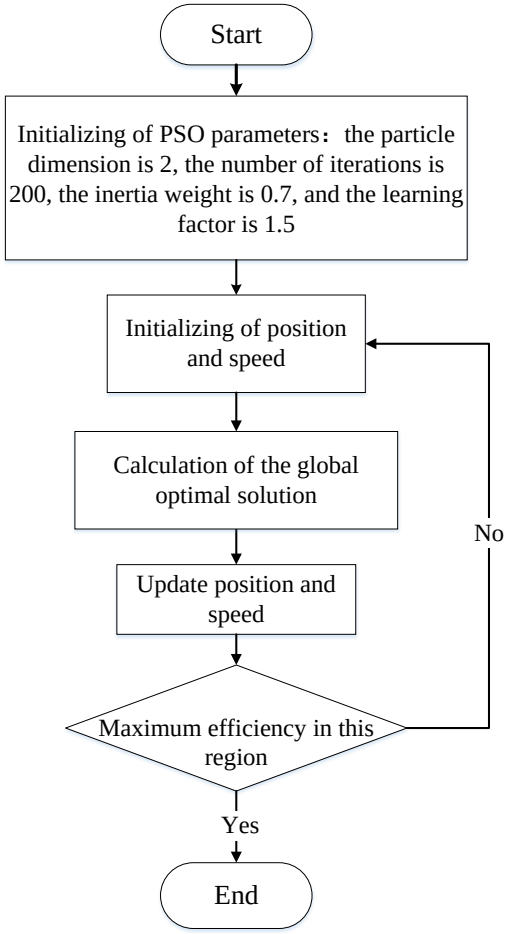

FIGURE 10. Matching capacitance and load optimization flow chart.

At the end of the iterative optimization search process, a set of C_3, R_L, and other parameter sets are obtained, along with the maximum transmission efficiency within this range. Additionally, the magnetic leakage at this point is derived by substituting the above parameters into Eqs. (6) to (9).

(4) Setting of judgment conditions: If the transmission efficiency is greater than 96% and the maximum magnetic leakage B on the observation surface less than 27 μT, save the result output; otherwise return to step (1) Re-optimize.

4.2. Optimization Results

According to the optimization in Subsection 4.1, the coil sizing parameters of the RMSDT structure are derived as shown in Table 1, and b_1, b_2, and b_3 are all 2 cm.

Using the parameters in Table 1, the coil model simulation diagram is drawn in Ansys Maxwell software. Simultaneously, the PSO process detailed in Subsection 4.1 is utilized to deter-

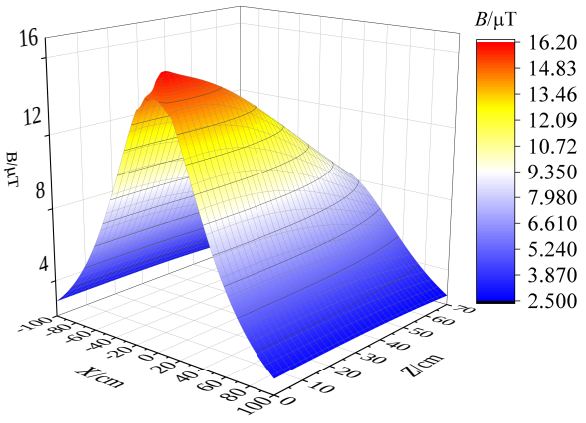

FIGURE 11. RMSDT system theoretically value distribution of magnetic leakage.

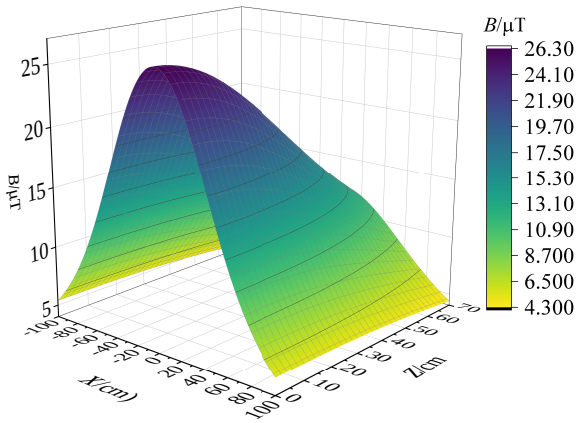

FIGURE 12. Conventional system theoretically value distribution of magnetic leakage.

TABLE 1. Parameters of coils.

Coils	Inner length/ cm	Inner width/cm	Turns
T_{x1}	48.00	19.00	15
T_{x2}	48.00	19.00	15
S_{C1}	63.00	7.00	2
S_{C2}	63.00	7.00	2
S_{C3}	80.00	7.00	2
S_{C4}	80.00	7.00	2
R_x	52.00	48.00	15
T'_x	68.00	68.00	15
R'_x	68.00	68.00	15

mine the optimal C_3 and R_L, which are found to be 1 nF and 30 Ω, respectively. The transmission efficiency of the RMSDT system is calculated to be 97.81%. In contrast, the traditional optimization method using a for-loop algorithm yields a peak transmission efficiency of 93.24%. Therefore, it is concluded that the PSO algorithm is highly effective in maintaining high transmission efficiency.

In order to visualize the shielding effect of the RMSDT structure, this paper compares it with a conventional WPT structure. To control variables, the number of turns is kept constant at 15 for both systems. Additionally, the inner width and length of the comparison group's coils are adjusted to 68 cm, ensuring that the overall coil structure size closely matches that of the RMSDT system, as shown in Table 1.

After finalizing the coil size parameters of the two structures, R'_x is connected to a 30 Ω load, and the output power is controlled to be 3.7 kw, matching that of the RMSDT system. The magnetic leakage is observed on the same observation surface to assess the effect of the shielding system discussed in this paper. Both sets of parameters are substituted into Eqs. (6) to (9) to obtain the theoretical values of the systems' magnetic leakage. The three-dimensional magnetic field distribution of the RMSDT system is shown in Figure 11, and the three-dimensional magnetic field distribution of the conventional WPT system is shown in Figure 12. It can be observed that the maximum magnetic leakage of the RMSDT system is 16.2 μT, whereas the maximum magnetic leakage of the conventional WPT system is 26.3 μT. This demonstrates that the RMSDT structure can effectively reduce magnetic leakage.

5. EXPERIMENTAL VERIFICATION

To verify the safety and correctness of the proposed structure, two sets of 3.7 kW experimental platforms were built in the laboratory: an RMSDT system platform and a traditional WPT system platform, as shown in Figures 13(a) and (b). The main components of the experimental platforms include loads, a WT5000 power analyzer, an RT unitary inverter-rectifier module, oscilloscope, a physical model of the coil, a DC power supply, and an NF-5035S electromagnetic radiation analyzer.

5.1. Experimental Setup

Based on the parameters in Table 1, the coil structures of the RMSDT system and conventional WPT system are derived, and the physical drawing of these coils is shown in Figure 14. The transmission efficiency and magnetic leakage are experimentally compared to verify the effectiveness of the RMSDT system. The Litz copper wire used in this study consists of 800 strands of 0.1 mm wire, with a maximum current capacity of 31.41 A.

The experimental steps are specified as follows: firstly, the physical parameters of the coil structure are measured using an IM3536 impedance analyzer. The detailed physical parameters obtained from the experiment are presented in Table 2. Secondly, the current and voltage waveforms at the transmitting and receiving ends of the coil are observed using an oscilloscope to determine the resonance state. The voltage of the direct current source is then adjusted until the output power reaches 3.7 kW. The transmission efficiency of the system using a WT5000 power analyzer and the magnetic leakage on the target surface are measured using an NF-5035S EMF analyzer along with its accompanying MCS EMF analyzer software.

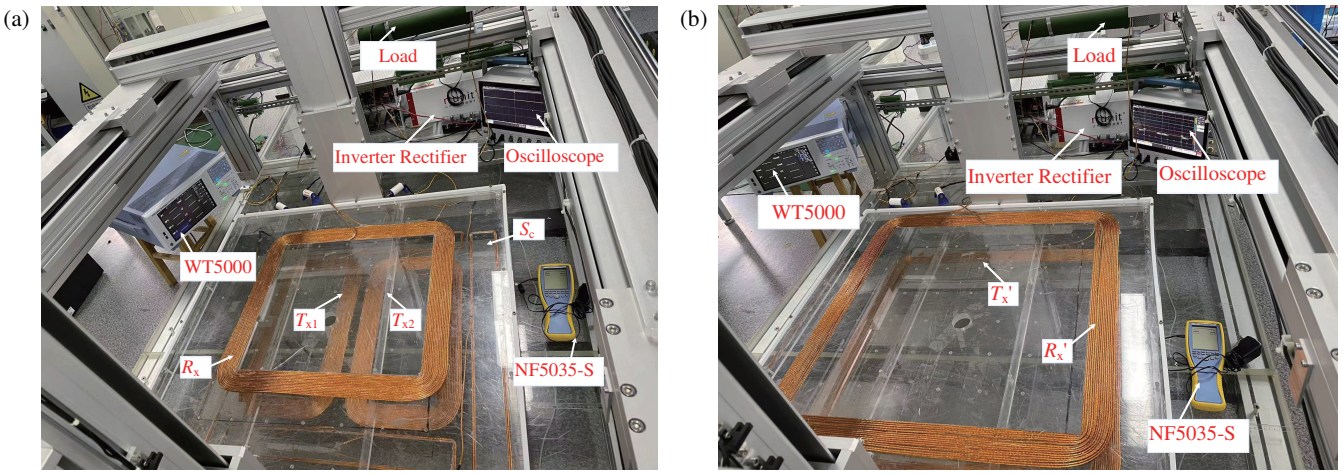

FIGURE 13. Experimental platforms. (a) RMSDT system platform. (b) Traditional WPT system platform.

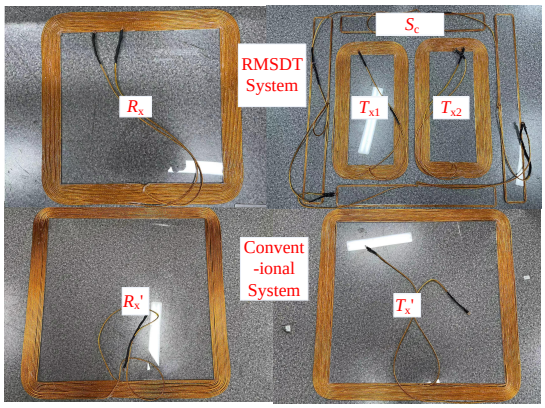

FIGURE 14. Physical diagram of coils.

TABLE 2. Physical parameters of the coils.

Parameter	Physical meaning	Value
L_1/μH	Self-inductance of T_{x1}	176
L_2/μH	Self-inductance of T_{x2}	179
L_3/μH	Self-inductance of S_c	17
L_4/μH	Self-inductance of R_x	292
L_1'/μH	Self-inductance of T_x'	424
L_2'/μH	Self-inductance of R_x'	429
C_1/nF	Resonant capacitance of T_{x1}	20
C_2/nF	Resonant capacitance of T_{x2}	20
C_3/nF	Optimal shielded coil matching capacitance	1
C_4/nF	Resonant capacitance of R_x	12
C_1'/nF	Resonant capacitance of T_x'	8
C_2'/nF	Resonant capacitance of R_x'	8
R_1/mΩ	Parasitic resistance of T_{x1}	188
R_2/mΩ	Parasitic resistance of T_{x2}	189
R_3/mΩ	Parasitic resistance of S_c	80
R_4/mΩ	Parasitic resistance of R_x	226
R_1'/mΩ	Parasitic resistance of T_x'	273
R_2'/mΩ	Parasitic resistance of R_x'	274
f_0/kHz	Operating frequency	85
R_L/Ω	Load	30

5.2. Magnetic Leakage of Systems

To test the effectiveness of the RMSDT system in reducing magnetic leakage, this subsection compares the magnetic leakage of the RMSDT system with that of the conventional WPT system.

When the output power of the system is constant at 3.7 kW, the following steps are performed to evaluate the leakage field condition: the distribution of the maximum magnetic leakage theoretical value B_c is obtained according to Subsection 4.2; the maximum magnetic leakage simulation value B_s is obtained using the finite element simulation software Ansys Maxwell; the results are shown in Figures 15(a) and (b); the maximum magnetic leakage experimental value B_e is measured using an EMR analyzer NF-5035S.

When parking, an electric vehicle may not be fully aligned with the parking space due to various reasons. This misalignment causes a change in the position of the coils, affecting their mutual inductance, weakening the effectiveness of magnetic leakage shielding. Therefore, it is necessary for us to study situations where the electric vehicle is offset from the charging device. In this experiment, the receiving coil is moved with the Y-axis direction to simulate the offset. Figures 16(a) and (b) show the variations of B_c, B_s, and B_e for the RMSDT system and conventional WPT system, respectively, when the receiving coil is shifted with the Y-axis direction. The error rates of both systems are below 7%, verifying the correctness of B_c and B_s.

Based on experimental results, when the system is aligned, the magnetic leakage of the RMSDT system is 16.08 μT, while the conventional WPT system exhibits a magnetic leakage of 27.36 μT. This indicates that the magnetic leakage is reduced by 41.8%. Furthermore, when the receiving coil is at different offsets, the magnetic leakage of the RMSDT system will still be significantly reduced compared to the conventional WPT system. Even at an offset of 100 mm, the magnetic leakage of the

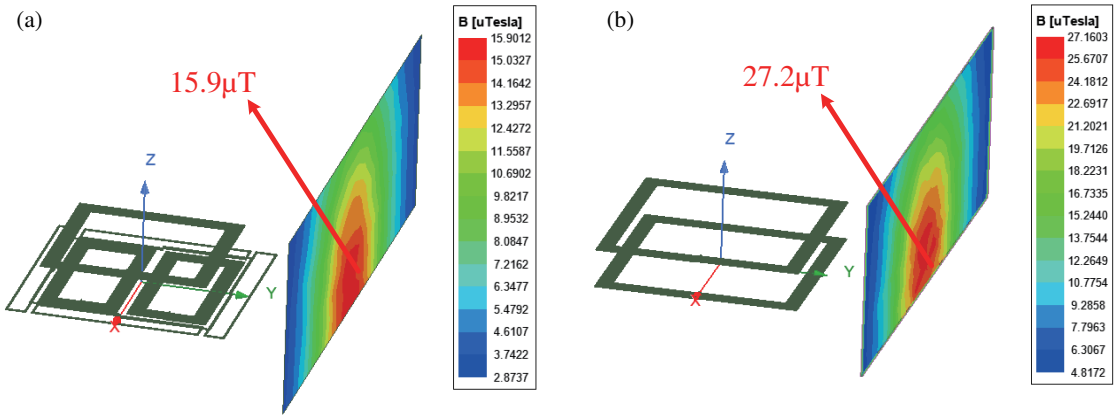

FIGURE 15. System simulation diagrams. (a) RMSDT system simulation value distribution of magnetic leakage. (b) Conventional system simulation value distribution of magnetic leakage.

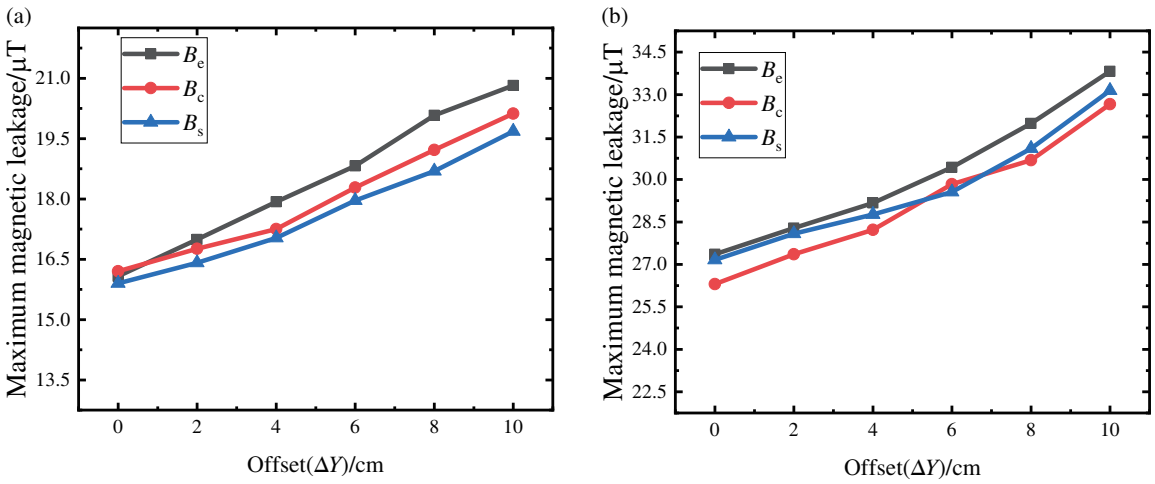

FIGURE 16. Magnetic leakage comparisons. (a) Magnetic leakage of the RMSDT system at different offset distances. (b) Magnetic leakage of the conventional system at different offset distances.

RMSDT system is 20.82 μT, representing a decrease of 38.4%, whereas the magnetic leakage of conventional WPT system is 33.91 μT.

Therefore, it can be found that the measured maximum magnetic leakage of the RMSDT system at any offset still meets the safety standard for human body, and it is substantially better than the measured maximum magnetic leakage of the conventional WPT system at the same distance of offset. As a consequence, it can be concluded that the structure has good anti-offset ability in reducing leakage magnetic field.

5.3. Transmission Efficiency of Systems

In order to measure system transmission efficiency when the receiving coil receives a constant power of 3.7 kW, the following steps are performed: the theoretical value of the transmission efficiency η_c is obtained through calculation; the simulation value η_s is obtained using Matlab/Simulink; and the experimental value of the transmission efficiency η_e is obtained using a Yokogawa WT5000 power analyzer.

As mentioned in Subsection 5.2, when the electric vehicle is parked, it will cause an offset which will cause a change in mutual inductance. As known by Eq. (15) and Eq. (19), mutual inductance will also cause changes in system transmission efficiency, so this subsection will study the performance of system transmission efficiency under the offset condition. To be specific, this subsection verifies the effectiveness of the RMSDT system by comparing its transmission efficiency with that of the conventional WPT system while offsetting the same distance.

Experiments show that when the system is aligned, transmission efficiency of the RMSDT system can reach 95.82%, and compared with the conventional WPT system, the RMSDT system effectively reduces 41.8% of magnetic leakage while sacrificing only 0.21% of transmission efficiency. This indicates that the coil structure of the RMSDT system can significantly reduce magnetic leakage while maintaining high transmission efficiency. Even with a 100 mm offset, the RMSDT system maintains a high transmission efficiency of 93.68%. Compared to the conventional WPT system with a 100 mm offset, the RMSDT system greatly reduces magnetic field leakage by 38.44%, and the efficiency loss of 0.29% is negligible.

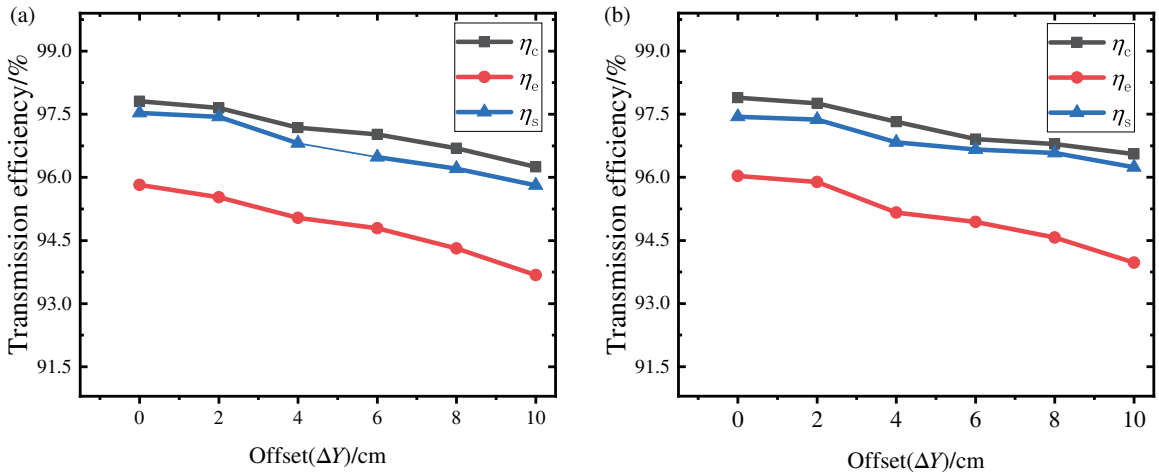

FIGURE 17. Transmission efficiency comparisons. (a) Transmission efficiency of RMSDT system at different offset distances. (b) Transmission efficiency of conventional system at different offset distances.

TABLE 3. Comparison of different existing magnetic shielding solutions.

Documentary sources	Shielding method	Shielding efficiency	Transmission efficiency
[26]	Reactive resonance shielding	21%	68.46%
[25]	Passive shieding+Al	21%	92.09%
[33]	Reactive resonance shielding	30.8%	\
This paper	Without source coils	41.8%	95.82%

As mentioned in Subsection 4.2, this paper employs the PSO algorithm for optimization, which can improve transmission efficiency by 4.63% compared to the traditional for-loop optimization process. Therefore, this subsection compares the transmission efficiency of the RMSDT system structure under the PSO algorithm and the for-loop optimization process, respectively, when offsetting the same distance, to validate the efficacy of the PSO algorithm in enhancing transmission efficiency.

Specifically, in this paper, the for-loop algorithm is utilized to play a role of comparison. To control the variables, both the PSO algorithm and for-loop algorithm optimize the same parameters, namely the optimal matching capacitance of shielding coil and the optimal load at receiving end. Meanwhile, the coil structure also uses the RMSDT structure to ensure that the two algorithms can be better compared. Then, the optimized transmission efficiency is calculated according to the same method as in Section 4. From the experiment, when the system is without offset, it is observed that the transmission efficiency of the system after the for-loop algorithm optimization is 91.06%, while another can reach 95.82% as mentioned before, so the PSO optimization can improve transmission efficiency by 4.76% compared with the for-loop optimization. Even with a 100 mm offset, the PSO algorithm can make the transmission efficiency reach 93.68% as mentioned before, which means increasing the transmission efficiency by 5.01% while the optimized transmission efficiency by the for-loop algorithm is only 88.67%. This demonstrates that the PSO algorithm is highly effective in improving the transmission efficiency of the system during optimization process.

Consequently, without offset, the transmission efficiency of the RMSDT system optimized by the PSO algorithm can reach 95.82%. Even with a 100 mm offset, the system can still achieve a high transmission efficiency of 93.68%, which shows that the RMSDT system has a good ability to cope with the impact of offset on maintaining high transmission efficiency. Compared to the conventional coil structure, the RMSDT structure significantly reduces magnetic leakage with almost no loss in transmission efficiency, so the RMSDT structure is clearly a better choice. Additionally, compared to the for-loop optimization method, the PSO algorithm improves the transmission efficiency of the same coil structure by 4.76% when the system is aligned, and there are also considerable improvements in different distances of offset, hence the PSO algorithm is a good way for optimization. The above efficiency change curves are shown in Figures 17(a), (b) and 18.

5.4. Performance Comparison

In summary, after comparing the RMSDT structure and conventional structure through experiments, this paper concludes that the RMSDT system mechanism presented here can achieve better shielding effects; then, after comparing the PSO algorithm and for-loop algorithm through experiments, it is also concluded that the WPT system can achieve a higher transmission efficiency when being optimized using the PSO algorithm.

This subsection compares the shielding method proposed in this paper with other studies. It includes shielding method, shielding efficiency, and transmission efficiency. The results are shown in Table 3. It shows that the structure proposed in

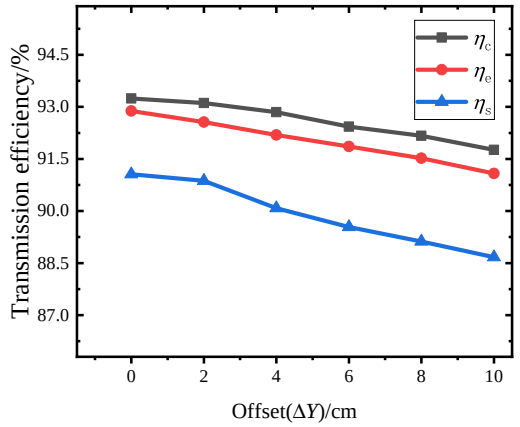

FIGURE 18. Transmission efficiency of the RMSDT system optimized by for-loop algorithm at different offset distances.

this paper has good magnetic shielding performance and transmission efficiency.

6. CONCLUSION

In this paper, a dual-transmitter coil ring-series magnetic shielding structure is proposed. The main feature of this structure is a dual-transmitting coil system, which incorporates a ring-series passive shielding coil that generates a reversed counteracting magnetic field to attenuate leakage magnetism in the region. For comparison, a conventional WPT system model is introduced, with the number of turns and overall dimensions set to match those of the proposed system (RMSDT system). Additionally, a coil parameter optimization method based on the PSO algorithm is applied to optimize the shielding coil matching capacitance as well as the load at the receiving end. This optimization ensures that transmission efficiency is maximized while the system leakage remains within human body safety standards. The optimized parameters are then used to determine the transmission efficiency and magnetic leakage values at the target transmission power. Experiments demonstrate that, compared to the conventional WPT system structure, the RMSDT structure reduces magnetic leakage by 41.8%, while maintaining a system transmission efficiency of over 95%. Furthermore, the PSO algorithm improves transmission efficiency by more than 4% compared with the traditional for-loop optimization method. Considering the vehicle's offset within a parking space, this paper investigates the shielding effect and transmission efficiency when the vehicle is offset along the Y-axis by up to 100 mm. Results show that even at the maximum offset, the magnetic leakage complies with human safety standards and maintains over 93% transmission efficiency. In conclusion, the RMSDT structure and the optimization method based on PSO algorithm effectively enhance the safety and efficiency of the system. Future research should prioritize simplifying the structural design and reducing the costs of wireless power transfer systems, and these advancements should be achieved without compromising the safety and efficiency of the systems.

ACKNOWLEDGEMENT

This work was supported in part by the Natural Science Foundation of Hunan Province under Grants 2022JJ30226, National Key R&D Program Project (2022YFB3403200), Key Projects of Hunan Provincial Department of Education (23A0432), and in part by Excellent Youth Project of Scientific Research of Hunan Provincial Department of Education (22B0577), National Natural Science Foundation of China (NSFC) Youth Science Fund Project (62303178) and A Project Supported by Scientific Research Fund of Hunan Provincial Education Department (23C0182).

REFERENCES

[1] Dou, R. T., X. Zhang, Y. J. Li, *et al.*, "Review on the application development and research of electromagnetic shielding of magnetically coupled resonant wireless power transfer system," *Proceedings of the CSEE*, Vol. 43, No. 15, 6020–6040, 2023.

[2] Yu, Z., W. Xiao, B. Zhang, and D. Qiu, "Development status of electric-field coupled wireless power transmission technology," *Transactions of China Electrotechnical Society*, Vol. 37, 1051–1069, 2022.

[3] Su, Y., X. Wu, Y. Zhao, *et al.*, "Parameter optimization of electric-field coupled wireless power transfer system with complementary symmetric lcc resonant network," *Transactions of China Electrotechnical Society*, Vol. 34, 2874–2883, 2019.

[4] Zhang, B., X. Shu, L. Wu, and C. Rong, "Problems of wireless power transmission technology urgent to be solved and corresponding counter measures," *Automation of Electric Power Systems*, Vol. 43, 1–12, 2019.

[5] Zhao, Z., Y. Zhang, and K. Chen, "New progress of magnetically-coupled resonant wireless power transfer technology," *Proceedings of the CSEE*, Vol. 33, No. 3, 1–13, 2013.

[6] Brown, W. C., "The history of power transmission by radio waves," *IEEE Transactions on Microwave Theory and Techniques*, Vol. 32, No. 9, 1230–1242, 1984.

[7] Huang, X., L. Tan, Z. Chen, H. Qiang, Y. Zhou, W. Wang, and W. Cao, "Review and research progress on wireless power transfer technology," *Transactions of China Electrotechnical Society*, Vol. 28, No. 10, 1–11, 2013.

[8] Su, L. and C. Zhou, "Review on the application development and research of electromagnetic shielding of magnetically coupled resonant wireless power transfer system," *World SCI-TECH R&D*, Vol. 35, 177–180, 2013.

[9] Zhang, J.-H., X.-L. Huang, Y.-W. Zou, and Y. Bai, "Feasibility of ultrasonic wireless power transmission," *Advanced Technology of Electrical Engineering and Energy*, Vol. 30, 66–69, 2011.

[10] He, X., Y. Zeng, R. Liu, C. Lu, C. Rong, and M. Liu, "A dual-band coil array with novel high-order circuit compensation for shielding design in ev wireless charging system," *IEEE Transactions on Industrial Electronics*, Vol. 71, No. 3, 2545–2555, 2024.

[11] Ge, H. and J. Qiu, "Research on improvement of anti-misalignment characteristics of static wireless charging system for electric vehicles based on relay coil," *Journal of Power Supply*, Vol. 21, 35–42, 2023.

[12] Wu, L. and B. Zhang, "Overview of static wireless charging technology for electric vehicles: Part I," *Tansactions of China Electrotechnical Society*, Vol. 35, No. 6, 1153–1165, 2020.

[13] Yang, Q., H. Chen, G. Xu, M. Sun, and W. Fu, "Research progress in contactless power transmission technology," *Diangong Jishu Xuebao/Transactions of China Electrotechnical Society*, Vol. 25, No. 7, 6–13, 2010.

[14] Campi, T., S. Cruciani, V. D. Santis, and M. Feliziani, "EMF safety and thermal aspects in a pacemaker equipped with a wireless power transfer system working at low frequency," *IEEE Transactions on Microwave Theory and Techniques*, Vol. 64, No. 2, 375–382, 2016.

[15] Dickinson, R. M., "Safety issues in SPS wireless power transmission," *Space Policy*, Vol. 16, No. 2, 117–122, 2000.

[16] Kurs, A., A. Karalis, R. Moffatt, J. D. Joannopoulos, P. Fisher, and M. Soljacic, "Wireless power transfer via strongly coupled magnetic resonances," *Science*, Vol. 317, No. 5834, 83–86, 2007.

[17] Hirayama, H., T. Amano, N. Kikuma, and K. Sakakibara, "A consideration of open- and short-end type helical antennas for magnetic-coupled resonant wireless power transfer," in *2012 6th European Conference on Antennas and Propagation (EUCAP)*, Prague, Czech Republic, May 2012.

[18] Jeong, S., D.-H. Kim, J. Song, H. Kim, S. Lee, C. Song, J. Lee, J. Song, and J. Kim, "Smartwatch strap wireless power transfer system with flexible PCB coil and shielding material," *IEEE Transactions on Industrial Electronics*, Vol. 66, No. 5, 4054–4064, 2019.

[19] Kim, J., J. Ahn, S. Huh, K. Kim, and S. Ahn, "A coil design and control method of independent active shielding system for leakage magnetic field reduction of wireless UAV charger," *IEICE Transactions on Communications*, Vol. E103-B, No. 9, 889–898, 2020.

[20] Ahn, J., J. Kim, D. Park, H. Kim, and S. Ahn, "An active shielding control method for a wireless power transfer system under misalignment conditions," *Journal of Electromagnetic Engineering and Science*, Vol. 22, No. 1, 56–63, 2022.

[21] Shen, D., G. P. Du, D. Y. Qiu, and B. Zhang, "Research status and development trend of electromagnetic compatibility of wireless power transmission system," *Transactions of China Electrotechnical Society*, Vol. 35, 2855–2869, 2020.

[22] Chen, C., X. Huang, L. Tan, F. Wen, and W. Wang, "Electromagnetic environment and security evaluation for wireless charging of electric vehicles," *Transactions of China Electrotechnical Society*, Vol. 30, No. 19, 61–67, 2015.

[23] Zhang, X., B. Li, L. Ren, P. Kong, and Z. Li, "Calculation and optimization of magnetic leakage in electric vehicle WPT based on bidirectional inverse series coils of four meshes," *Progress In Electromagnetics Research M*, Vol. 123, 105–117, 2024.

[24] Zhang, X., L. Ren, P. Kong, X. Xiong, and Z. Li, "Study of a double-layer passive magnetic shielding system for electric vehicle WPT," *Progress In Electromagnetics Research C*, Vol. 137, 65–79, 2023.

[25] Mohammad, M., E. T. Wodajo, S. Choi, and M. E. Elbuluk, "Modeling and design of passive shield to limit EMF emission and to minimize shield loss in unipolar wireless charging system for EV," *IEEE Transactions on Power Electronics*, Vol. 34, No. 12, 12 235–12 245, 2019.

[26] Lee, S., D.-H. Kim, Y. Cho, H. Kim, C. Song, S. Jeong, J. Song, G. Park, S. Hong, J. Park, *et al.*, "Low leakage electromagnetic field level and high efficiency using a novel hybrid loop-array design for wireless high power transfer system," *IEEE Transactions on Industrial Electronics*, Vol. 66, No. 6, 4356–4367, 2019.

[27] Campi, T., S. Cruciani, F. Maradei, and M. Feliziani, "Magnetic field mitigation by multicoil active shielding in electric vehicles equipped with wireless power charging system," *IEEE Transactions on Electromagnetic Compatibility*, Vol. 62, No. 4, 1398–1405, 2020.

[28] Huh, S., J. Park, S. Lee, K. Kim, S. Woo, C. Lee, J. Rhee, S. Son, and S. Ahn, "Design of reactive shield coil for wireless charger with multiple coils," in *2021 IEEE Wireless Power Transfer Conference (WPTC)*, 1–4, San Diego, CA, USA, Jun. 2021.

[29] Choi, S., S. Huh, S. Woo, H. Kim, J. Kim, G. Jung, K. A. Hosani, and S. Ahn, "EMF reduction method considering efficiency degradation using two reactive shielding coils in multi-transmitter wireless power transfer system," in *2022 Wireless Power Week (WPW)*, 60–63, Bordeaux, France, Jul. 2022.

[30] Liu, T. Z. and Z. H. Zhang, "Online identification of joint parameters of electric vehicle wireless charging system based on loop-iteration particle swarm optimization," *Transactions of China Electrotechnical Society*, Vol. 37, 4548–4564, 2022.

[31] Li, Z. Q., J. Li, C. H. Quan, X. Y. Zhang, S. D. Huang, *et al.*, "Mutual inductance calculation of arbitrarily positioned rectangular coils with magnetic shielding in wireless power transfer systems," *Transaction of China Electrotechnical Society*, Vol. 37, No. 17, 4294–4305, 2022.

[32] Li, Z., X. Xiong, P. Kong, and L. Ren, "Research on electromagnetic shielding and efficiency optimization technology of wireless power transfer system," *Journal of Electronic Measurement and Instrumentation*, Vol. 37, No. 5, 151–162, 2023.

[33] Kim, S., H.-H. Park, J. Kim, J. Kim, and S. Ahn, "Design and analysis of a resonant reactive shield for a wireless power electric vehicle," *IEEE Transactions on Microwave Theory and Techniques*, Vol. 62, No. 4, 1057–1066, 2014.